

Mapping phases of singular scalar light fields

Vladimir G. Denisenko,^{1,2} Alexander Minovich,¹ Anton S. Desyatnikov,^{1,*} Wieslaw Krolikowski,³
Marat S. Soskin,² and Yuri S. Kivshar¹

¹Nonlinear Physics Center, Australian National University, Canberra, ACT 0200, Australia

²Institute of Physics, National Academy of Science of Ukraine, 46 Prospekt Nauki, Kiev-39, 03650, Ukraine

³Laser Physics Center, Australian National University, Canberra, ACT 0200, Australia

*Corresponding author: asd124@rsphysse.anu.edu.au

Received November 2, 2007; revised November 25, 2007; accepted November 26, 2007;
posted November 28, 2007 (Doc. ID 89287); published December 21, 2007

We implement experimentally a simple method for accurate measurements of phase distributions of scalar light fields. The method is based on the polarimetric technique for recording the polarization maps of vector fields, where coaxial superposition of orthogonally polarized reference and signal beams allows the signal phase to be reconstructed from the polarization map of the total field. We demonstrate this method by resolving topologically neutral pairs of closely positioned vortices in a speckle field and recovering the positions of vortices within a Laguerre–Gaussian beam with the topological charge three. © 2007 Optical Society of America

OCIS codes: 050.4865, 260.5430, 260.6042.

Intricate light fields, including speckle fields, can be regarded as superpositions of many partial waves no matter how they are obtained: interference, reflection, or diffraction. An intensity distribution with alternating dark and bright spots indicates the necessity of a large number of modes for the pattern analysis. Furthermore, the phase front of a uniformly polarized (scalar) speckle field is singular; i.e., it contains screw-type phase dislocations (singularities) in the low-intensity regions [1]. A common method to visualize phase singularities is based on interference with a tilted plane wave; the characteristic fork-type bifurcations of the interferometric fringes indicate the positions of the phase singularities [2].

An example of the complex scalar field with a non-trivial phase structure is an optical vortex, e.g., a doughnutlike Laguerre–Gaussian LG_{m0} mode with a dark spot at its center surrounded by a bright ring. At the vortex core the phase contains a screw dislocation with the winding number m (also called the vortex topological charge). The interferometric analysis allows one to determine the presence of isolated phase defects, as well as to locate their positions with an accuracy no better than half the width of the interference fringe. However, the application of this method is rather limited if there are two (or more) dislocations in close proximity, because two vortices can be successfully resolved only if they are separated, in the absence of noise, by at least by one full fringe.

In this Letter, we demonstrate a different method for reconstructing the phase structure of light fields, originally suggested by Freund [3]. The method is based on measuring the Stokes parameters of the elliptically polarized vector field, and it was employed earlier [4] to measure the phase distribution around a single optical vortex generated by a computer-synthesized hologram [5,6]. Here we elaborate this approach and compare it with the interferometric technique in the case of a speckle pattern carrying randomly positioned optical vortices, and we also apply this method to resolve the phase structure of a

triple-charge vortex carried by the LG_{30} mode. We show that, while the interferometric method allows one to determine correctly the total topological charge of the complex field, it fails to resolve its fine phase structure. We believe that the method described here can be useful in a broad range of experimental situations where a fine structure of the wave front plays an important role.

A uniformly polarized light field can be measured in the basis of linear polarizations. Therefore, to map the unknown phase of a scalar signal wave, we assume it, without loss of generality, to be linearly polarized along the x direction, E_x , and superimpose it coaxially with an orthogonally polarized reference wave E_y , where

$$\begin{aligned} E_x &= A_x \cos(\Phi_1 + \omega t), \\ E_y &= A_y \cos(\Phi_2 + \omega t). \end{aligned} \quad (1)$$

The total field $\mathbf{E} = \mathbf{x}E_x + \mathbf{y}E_y$ is elliptically polarized, and the vibrational phase is given by $\delta = \Phi_1 - \Phi_2$. With respect to the propagation direction z , the polarization ellipse is left-handed for $-\pi < \delta < 0$ and right-handed for $0 < \delta < \pi$. The so-called L lines of pure linear polarization appear where the phase δ equals an integer multiple of π , while the isolated C points of pure circular polarization correspond to the degenerate case $A_x = A_y$ and $\delta = \pi/2 + n\pi$, $n = 0, \pm 1, \pm 2, \dots$

We employ Stokes parameters to describe the elliptically polarized field (see Sec. 10.8.3 in [7]),

$$\begin{aligned} S_0 &= A_x^2 + A_y^2, & S_1 &= A_x^2 - A_y^2, \\ S_2 &= 2A_x A_y \cos \delta, & S_3 &= 2A_x A_y \sin \delta, \end{aligned} \quad (2)$$

so that the phase difference is simply $\delta = \tan^{-1}(S_3/S_2)$. The measurement of the Stokes parameters is a straightforward task using methods of Stokes polarimetry; see [8–11] and the setup in Fig. 1. To determine the phase difference between the ref-

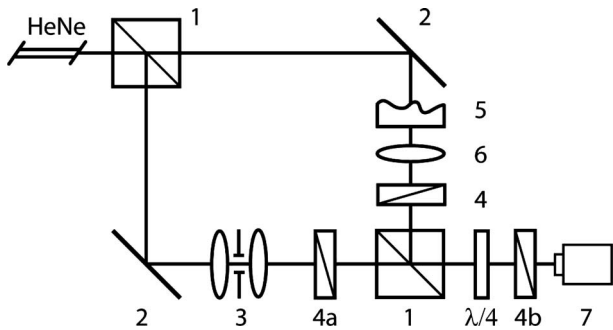


Fig. 1. Experimental setup: 1, beam splitters; 2, mirrors; 3, collimator with the diaphragm; 4, polarizers; 5, sample; 6, collimating lens; 7, CCD camera.

erence and the signal waves, one needs only two parameters [4]:

$$S_2 = I(45, 45) - I(135, 135),$$

$$S_3 = I(45, 0) - I(135, 0), \quad (3)$$

where $I(\alpha, \beta)$ is the intensity measured with polarizer-analyzer 4b (see Fig. 1) tilted at the angle α and the $\lambda/4$ plate is tilted at the angle β . This definition of the Stokes parameters ensures cancellation of a common background in the intensity measurements, improving their accuracy significantly. Since the reconstruction of the signal phase Φ_1 from the measured distribution of $\delta(x, y)$ requires known reference phase Φ_2 , it is most convenient to choose a simple reference wave, e.g., a plane wave with $\Phi_2 = \text{constant}$ or a Gaussian beam at its waist. Note that the amplitude variations of the reference beam do not influence the accuracy of the phase measurements.

Vortices in speckle fields. We first apply this method to characterize the phase of a speckle field obtained by diffraction on a double-side randomly rubbed glass plate (sample 5 in Fig. 1). The intensity distribution of a small part of the generated field is shown in Fig. 2(a). We see clearly at least six maxima and four dark minima, the latter suggesting the presence of intensity zeros or optical vortices. The interference pattern shown in Fig. 2(b) confirms this assumption; in particular, counting the number of fringes at the top (14) and the bottom (15) boundaries, we can calculate a nonzero total topological charge ($14 - 15 = -1$). Furthermore, the bottom center region, marked “A” in Fig. 2(a), contains a pair of fork bifurcations oriented in opposite directions, indicating the presence of two vortices of opposite charges separated by the distance $\sim 250 \mu\text{m}$. The results of polarimetric measurements of the phase front shown in Figs. 2(c) and 2(d) simply confirm this conclusion.

In contrast to the clearly visible region A, the interference diagram in Fig. 2(b) does not allow us to draw any conclusions about deformed fringes in regions B (top right) and C (top left). These regions represent two distinct cases where our method shows an advantage over the traditional interferometric measurements. Indeed, while in both cases a topologically neutral (charge zero) region of strongly deformed fringes appears in Fig. 2(b), only by following the

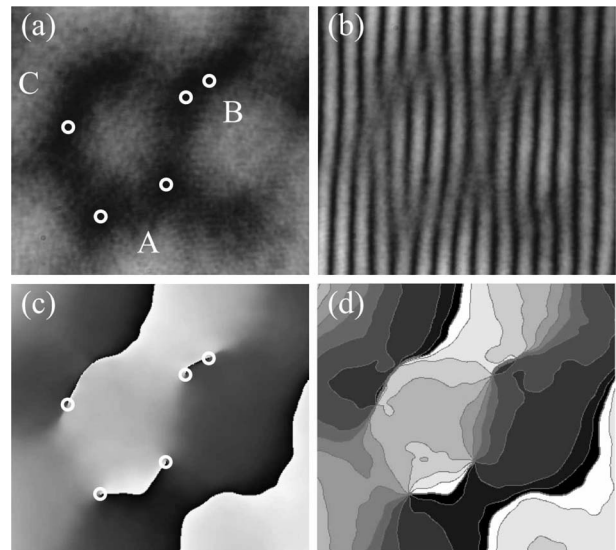


Fig. 2. (a) Intensity, (b) interference pattern, and (c), (d) phase of a speckle field. Circles indicate the positions of vortices, and lines in (d) illustrate deformations of phase contours around the dislocations. The phase surface in (c) and (d) is gray coded from $-\pi$ (black) to π (white).

phase profile reconstructed in Figs. 2(c) and 2(d) can we distinguish the presence of a vortex-antivortex pair [12] in region B and its absence in region C. In the latter case the presence of an antivortex is identified in the interference picture above, while its position could be traced in Fig. 2(c) only because of a strong deformation of the phase contour lines [13–15]; see Fig. 2(d).

Fine structure of a triple-charge vortex. We now consider the other example where fine details of the phase structure can be crucial for the distinction between topologically different light fields, namely, the modes with higher-order topological charge [2, 15, 16]. As is known, the family of the Laguerre-Gaussian beams includes higher-order phase dislocations, $E_m \sim r^{|m|} \exp(im\varphi)$ with the angular variable φ and topological charge m . However, all modes with $|m| > 1$ are nongeneric, or structurally unstable [17]. This means that a small perturbation may transform a point phase defect into several spatially separated single-charge vortices. Ideally, the number of single-charge vortices coincides with m , but it can also include additional topologically neutral pairs.

Using two methods described above we measure the interference pattern of a hologram-generated triple-charge vortex beam, shown in Fig. 3(a), and its phase, shown in Fig. 3(b). The visibility of the interference fringes at the center of the vortex is very low because the vortex intensity decays as $\sim r^{2|m|}$ when $r \rightarrow 0$. As a result, while the number of the fringes on the top and bottom of Fig. 3(a) allows us to determine the total topological charge to be three, there is no way to determine the number and positions of phase dislocations. In contrast, the polarimetric measurement of Fig. 3(b) shows three well-separated single-charge vortices, with the distance from the top vortex to the bottom one $\sim 500 \mu\text{m}$.

The vanishing amplitude at the vortex core sets a lower bound to the whole region around a dislocation

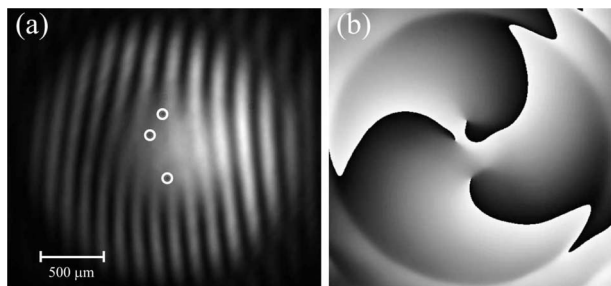


Fig. 3. (a) Interference pattern and (b) phase of a vortex beam with topological charge three; circles mark the positions of three single-charge vortices.

for which the interferometric technique is able to visualize the phase profile. Indeed, in accordance with the Michelson criterion (see Sec. 7.3.4 in [7]), two fringes can be resolved by eye if the visibility parameter exceeds 10%, $V > 0.1$, where $V = (I_{\max} - I_{\min}) / (I_{\max} + I_{\min})$. Thus, the resolution is successful only in the regions where the minimum intensity I_{\min} is below a certain threshold, namely, $I_{\min} < 0.82I_{\max}$. For coherent superposition of a vortex with the intensity I_{OV} and a broad Gaussian beam (plane wave) with the intensity I_G , we obtain $I_{\max} = I_G + I_{OV}$ and $I_{\min} = |I_G - I_{OV}|$. Thus, close to the vortex origin with $I_G > I_{OV}$, the interference fringes can be resolved if $I_{OV} > 0.1I_G$, and this condition cuts out the region containing phase dislocations. More specifically, the intensity of an ideal Laguerre–Gaussian vortex with the charge m (including a Gaussian beam at $m=0$) is given by $I_m \sim (r/w)^{2|m|} \exp(-2r^2/w^2)$, where w is the waist parameter. Thus, for the superposition of two beams the condition $I_m > 0.1I_0$ implies that the visibility of the interference fringes exceeds the threshold provided that $r/w > 10^{-1/2|m|}$. The dark region quickly grows with m , e.g., $r/w > 0.314$ for $m=1$, ~ 0.562 for $m=2$, and it is ~ 0.681 for $m=3$. Thus, for a single-charge beam with the waist $w=1$ mm, the dark core out of contrast will be a spot with the size $\sim 314 \mu\text{m}$. In speckle fields such dark spots will be smaller because of stronger gradients of intensity, but the order of magnitude will be the same.

We point out that the reconstruction of the phase profile is possible by using phase-shifting interferometry [18] requiring precise control over the phase of the reference wave and complicated algorithms for postprocessing. Furthermore, any small fluctuations of the phase difference lead to additional shifts of fringes and bring an intrinsic error in the measurements of vortex positions. At the theoretical limit of resolution of two binary interference fringes necessary to detect a phase singularity, one needs at least 4 pixels at the CCD camera; in practice this number is ~ 10 pixels. Thus, with a typical pixel size of

$4.4 \mu\text{m}$, the location of a vortex can be determined with an accuracy not exceeding $\sim 50 \mu\text{m}$. In contrast, the coaxial polarimetric scheme can, in principle, deliver a resolution of phase as high as $\lambda/100$, although it is also limited by the finite dynamical range of the intensity measurements.

In conclusion, we have verified experimentally a simple method for accurate measurements of scalar optical fields carrying phase singularities (optical vortices). This method utilizes coaxial polarimetric techniques, and it brings essential advantages over the traditional methods based on interferometry. As an example of the application of this method, we have demonstrated how to resolve the positions of closely located optical vortices of opposite charges in a speckle pattern and also reconstructed a fine structure of the field phase in the vicinity of a dark core of a triple-charge vortex beam.

This work has been supported by the Discovery Project grant of the Australian Research Council.

References

1. J. F. Nye, *Natural Focusing and Fine Structure of Light* (Institute of Physics, 1999).
2. I. V. Basisty, B. Yu. Bazhenov, M. S. Soskin, and M. V. Vasnetsov, *Opt. Commun.* **103**, 422 (1993).
3. I. Freund, *Opt. Lett.* **26**, 1996 (2001).
4. V. G. Denisenko, V. V. Slyusar, M. S. Soskin, and I. Freund, *Asian J. Phys.* **15**, 199 (2006).
5. M. S. Soskin, M. V. Vasnetsov, and I. V. Basisty, *Proc. SPIE* **2647**, 57 (1995).
6. Z. S. Sacks, D. Rozas, and G. A. Swartzlander, Jr., *J. Opt. Soc. Am. B* **15**, 2226 (1998).
7. M. Born and E. W. Wolf, *Principles of Optics* (Pergamon, 1968).
8. V. G. Denisenko, G. A. Galich, V. V. Slyusar, and M. S. Soskin, *Ukr. J. Phys.* **48**, 594 (2003).
9. M. Soskin, V. Denisenko, and I. Freund, *Opt. Lett.* **28**, 1475 (2003).
10. M. Soskin, V. Denisenko, and R. Egorov, *J. Opt. A, Pure Appl. Opt.* **6**, S281 (2004).
11. V. G. Denisenko, R. Egorov, and M. S. Soskin, *Proc. SPIE* **5477**, 41 (2004).
12. G. Indebetouw, *J. Mod. Opt.* **40**, 73 (1993).
13. M. Vasnetsov and K. Stliunas, eds., *Optical Vortices*, Vol. 228 of Horizons in World Physics (Nova Science, 1999).
14. V. G. Denisenko, M. V. Vasnetsov, and M. S. Soskin, *Proc. SPIE* **4403**, 82 (2001).
15. L. Allen, S. M. Barnett, and M. J. Padgett, *Optical Angular Momentum* (Institute of Physics, 2003).
16. V. Y. Bazhenov, M. S. Soskin, and M. V. Vasnetsov, *J. Mod. Opt.* **39**, 985 (1992).
17. M. V. Berry, in *Physics of Defects*, Les Houches Session XXXV, R. Balian, M. Klman, and J.-P. Poirier, eds. (North-Holland, 1980), pp. 453–543.
18. K. Creath, in *Holographic Interferometry*, P. K. Rastogi, ed., Vol. 68 of Springer Series in Optical Science (Springer-Verlag, 1994), p. 109.